Linear Collider Test of a Neutrinoless Double Beta Decay Mechanism in left-right Symmetric Theories

James Barry[1*], Luis Dorame[1,2†], Werner Rodejohann[1‡]

[1]*Max-Planck-Institut für Kernphysik,*
Saupfercheckweg 1, 69117 Heidelberg, Germany

[2]*AHEP Group, Institut de Física Corpuscular – C.S.I.C./Universitat de València Edificio Institutos de Paterna, Apt 22085, E-46071 Valencia, Spain*

Abstract

There are various diagrams leading to neutrinoless double beta decay in left-right symmetric theories based on the gauge group $SU(2)_L \times SU(2)_R$. All can in principle be tested at a linear collider running in electron-electron mode. We argue that the so-called λ-diagram is the most promising one. Taking the current limit on this diagram from double beta decay experiments, we evaluate the relevant cross section $e^- e^- \to W_L^- W_R^-$, where W_L^- is the Standard Model W-boson and W_R^- the one from $SU(2)_R$. It is observable if the life-time of double beta decay and the mass of the W_R are close to current limits. Beam polarization effects and the high-energy behaviour of the cross section are also analyzed.

*E-mail: `james.barry@mpi-hd.mpg.de`
†E-mail: `dorame@ific.uv.es`
‡E-mail: `werner.rodejohann@mpi-hd.mpg.de`

arXiv:1203.3365v2 [hep-ph] 29 May 2012

1 Introduction

There are at present several experiments searching for neutrinoless double beta decay ($0\nu\beta\beta$) that are running, under construction or in the planning phase [1, 2]. Observation of $0\nu\beta\beta$ will be proof of lepton number violation, but extracting more specific information requires an assumption as to the underlying mechanism of the process. While one usually assumes that massive Majorana neutrinos will be the leading contribution, there are many other particle physics candidates that can lead to $0\nu\beta\beta$ [3, 4]. These include, to name a few, particles in R-parity violating supersymmetric theories, heavy (including fourth generation) neutrinos, leptoquarks, Majorons, as well as particles arising in extra-dimensional and left-right symmetric theories. Indeed, current limits on the lifetime of $0\nu\beta\beta$ can be used to set constraints on a variety of particle physics parameters [4]. In this paper we will focus on $0\nu\beta\beta$ within left-right symmetric theories, and propose to test one of the possible diagrams at a linear collider running in like-sign electron mode.

It is obvious that in comparison to $0\nu\beta\beta$ a linear collider has the advantage of providing an extremely clean environment to test lepton number violation. While $0\nu\beta\beta$,

$$(A, Z) \to (A, Z + 2) + 2e^- \,, \tag{1}$$

is plagued by nuclear physics uncertainties, linear collider processes such as

$$e^- e^- \to W^- W^- \tag{2}$$

directly test the central part of most $0\nu\beta\beta$-diagrams, see for instance Figs. 1, 2 and 3. Indeed, the process (2), often called inverse neutrinoless double beta decay, has been proposed frequently in the past [5–19] to test lepton number conservation and to check the mechanism of $0\nu\beta\beta$. Here we revisit the process in which left-handed and right-handed W-bosons of an $SU(2)_L \times SU(2)_R$ symmetric theory are produced [6, 9, 10]:

$$e^- e^- \to W_L^- W_R^- \,, \tag{3}$$

depicted in Fig. 4. The corresponding double beta diagram is the so-called λ-diagram, see Fig. 3(a). We will argue that from the many possible $0\nu\beta\beta$-diagrams in left-right symmetric theories, this is the one which promises the largest cross section at an electron-electron machine. We evaluate the cross section and apply current limits from $0\nu\beta\beta$ to it. Beam polarization issues are also considered, and the high energy behaviour of the cross section is analyzed.

Note that lepton number violating processes can be tested at hadron colliders via the process $q\bar{q}' \to \ell\ell jj$, i.e. production of like-sign dileptons plus jets, which could proceed via the exchange of heavy neutrinos and right-handed W bosons. Several studies in this direction have been performed [20–23], although the λ-diagram was not included[1]. Recent analyses by

---

[1]For other collider probes of $0\nu\beta\beta$, see [24, 25].

the CMS [26] and ATLAS [27, 28] collaborations using data from pp collisions at $\sqrt{s} = 7$ TeV have excluded certain regions in the $m_{W_R} - M_R$ mass plane, where M_R is the right-handed neutrino mass scale. The ATLAS limit on m_{W_R} extends up to nearly 2.5 TeV for some values of M_R, assuming that $m_{W_R} > M_R$. These analyses also assume negligible left-right mixing between light and heavy neutrinos and between gauge bosons.

Other features of the left-right symmetric model include the existence of a new neutral gauge boson Z', which could in principle be seen at both pp [21] and e^+e^- colliders [29] (see Ref. [30] for a review and further references). Roughly speaking, since $m_{Z'} \simeq 1.7 m_{W_R}$ (see Appendix A), the cross sections for processes such as $pp \to Z' \to \ell^+\ell^-$ will be lower than those involving charged gauge bosons. At linear colliders the Z' could mediate new four fermion interactions, i.e. $e^+e^- \to Z' \to f\bar{f}$, and could be detected due to interference with the virtual γ and Z contributions. In addition, the model includes doubly charged scalar bosons, which could be produced in pp and e^+e^- collisions [31, 32]; the latest ATLAS limits are $m_{\delta_L^{\pm\pm}} > 244$ GeV and $m_{\delta_R^{\pm\pm}} > 209$ GeV [33]. s-channel production of δ^{--} at like-sign linear colliders has been studied in, e.g. Refs. [34, 35].

The detection of a neutral gauge boson or doubly charged scalars would provide alternative tests of the left-right model, although the former has no immediate connection to $0\nu\beta\beta$. Here we focus on the λ-diagram at an e^-e^- machine, and show that it is observable if the W_R mass and the life-time of $0\nu\beta\beta$ are close to their current limits. Note that this process can be tested not only at a linear collider, but also due to its unique angular distribution in $0\nu\beta\beta$ [36], and that it has not yet been studied at hadron colliders. Our analysis is thus complementary to those in Refs. [20–23].

The paper is built up as follows: in Section 2 we summarize the various diagrams for $0\nu\beta\beta$ within left-right symmetric theories, and argue that the so-called λ-diagram looks most promising for tests at a linear collider. Then in Section 3 we discuss the cross section, including the effects of beam polarization. Details of left-right symmetric theories, a study of the high energy behaviour, and the helicity amplitudes of the process are delegated to the appendices, and we conclude in Section 4.

2 $0\nu\beta\beta$ in left-right symmetric models

Here we summarize the various possible diagrams for $0\nu\beta\beta$ in left-right symmetric models (for one of the first analyses on this topic, see [37]). Details of the theory are delegated to Appendix A; here it suffices to know that there are left- and right-handed currents with the associated gauge bosons W_L and W_R (that can mix with each other), Higgs triplets Δ_L and Δ_R coupling to left- and right-handed leptons, respectively, as well as light left-handed and heavy right-handed Majorana neutrinos that can also mix with each other. With this particle content, one can construct the diagrams leading to $0\nu\beta\beta$ displayed in Figs. 1, 2 and 3. They can be categorized in terms of their topology and the helicity of the final state electrons.
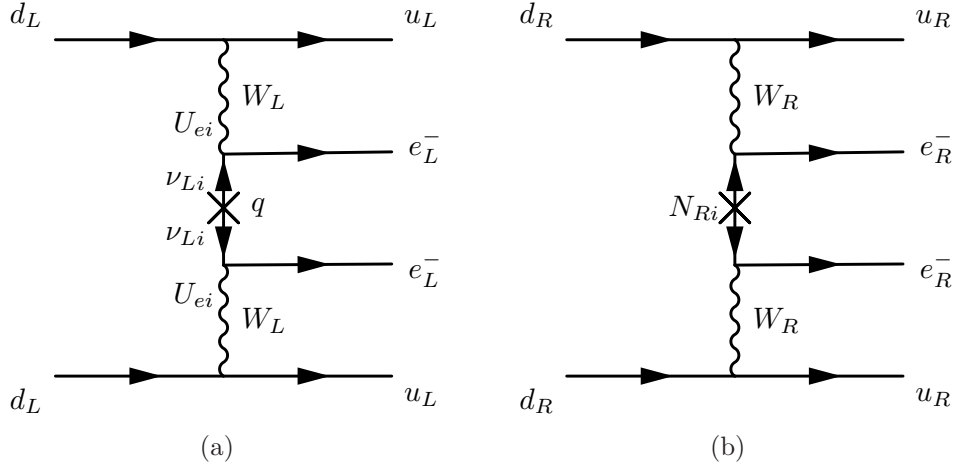
Figure 1: Feynman diagrams of double beta decay in the left-right symmetric model, mediated by (a) light neutrinos (the standard mechanism) and by (b) heavy neutrinos in the presence of right-handed currents. There is also a diagram with heavy neutrino exchange and left-handed currents, as well light neutrino exchange and right-handed currents, the latter is negligible.

We will discuss them in detail; the limits on the particle physics parameters are taken from Ref. [4].

- Fig. 1(a) is the standard diagram, whose amplitude is proportional to

$$\mathcal{A}_{LL} \simeq G_F^2 \frac{\langle m_{ee} \rangle}{q^2}, \tag{4}$$

where $|q^2| \simeq (100 \text{ MeV})^2$ is the momentum exchange of the process. The particle physics parameter $\langle m_{ee} \rangle \equiv |\sum U_{ei}^2 m_i|$ is called the effective mass, and the suitably normalized dimensionless parameter describing lepton number violation is

$$\eta_{LL} = \frac{\langle m_{ee} \rangle}{m_e} = \frac{|\sum U_{ei}^2 m_i|}{m_e} \lesssim 9.9 \times 10^{-7}. \tag{5}$$

Here U_{ei} is the (PMNS) mixing matrix of light neutrinos and m_i are the light neutrino masses.

- Fig. 1(b) is the exchange of right-handed neutrinos with purely right-handed currents. The amplitude is proportional to

$$\mathcal{A}_{N_R} \simeq G_F^2 \left(\frac{m_{W_L}}{m_{W_R}} \right)^4 \sum_i \frac{V_{ei}^{*2}}{M_i}, \tag{6}$$

where m_{W_R} (m_{W_L}) is the mass of the right-handed W_R (left-handed W_L), M_i the mass of the heavy neutrinos and V the right-handed analogue of the PMNS matrix U. The
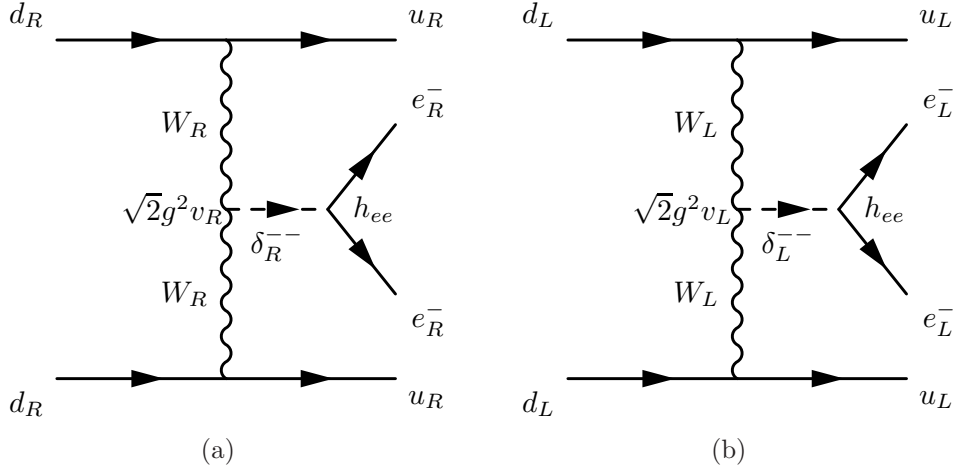
Figure 2: Feynman diagrams of double beta decay in the left-right symmetric model, mediated by doubly charged triplets: (a) triplet of $SU(2)_R$ and (b) triplet of $SU(2)_L$.

dimensionless particle physics parameter is

$$\eta_{N_R} = m_p \left(\frac{m_{W_L}}{m_{W_R}} \right)^4 \left| \sum_i \frac{V_{ei}^{*2}}{M_i} \right| \lesssim 1.7 \times 10^{-8} \,. \tag{7}$$

There is also a diagram with left-handed currents in which right-handed neutrinos are exchanged. The amplitude is proportional to

$$\mathcal{A}_{N_R^{(\mathrm{LH})}} \simeq G_F^2 \sum_i \frac{S_{ei}^2}{M_i} \,, \tag{8}$$

with S describing the mixing of the heavy neutrinos with left-handed currents. The limit is

$$\eta_{N_R^{(\mathrm{LH})}} = m_p \left| \sum_i \frac{S_{ei}^2}{M_i} \right| \lesssim 1.7 \times 10^{-8} \,. \tag{9}$$

Another possible diagram is light neutrino exchange with right-handed currents, which is however highly suppressed.

- Fig. 2(a) is a diagram with different topology, mediated by the triplet of $SU(2)_R$. The amplitude is given by

$$\mathcal{A}_{\delta_R} \simeq G_F^2 \left(\frac{m_{W_L}}{m_{W_R}} \right)^4 \sum_i \frac{V_{ei}^{*2} M_i}{m_{\delta_R^{--}}^2} \,, \tag{10}$$

and the dimensionless particle physics parameter is

$$\eta_{\delta_R} = \frac{\left| \sum_i V_{ei}^{*2} M_i \right|}{m_{\delta_R^{--}}^2 m_{W_R}^4} \frac{m_p}{G_F^2} \lesssim 6.9 \times 10^{-6} \,. \tag{11}$$

Here we have used the fact that the term $v_R h_{ee}$ is nothing but the ee element of the right-handed Majorana neutrino mass matrix M_R diagonalized by V, with v_R the VEV

5
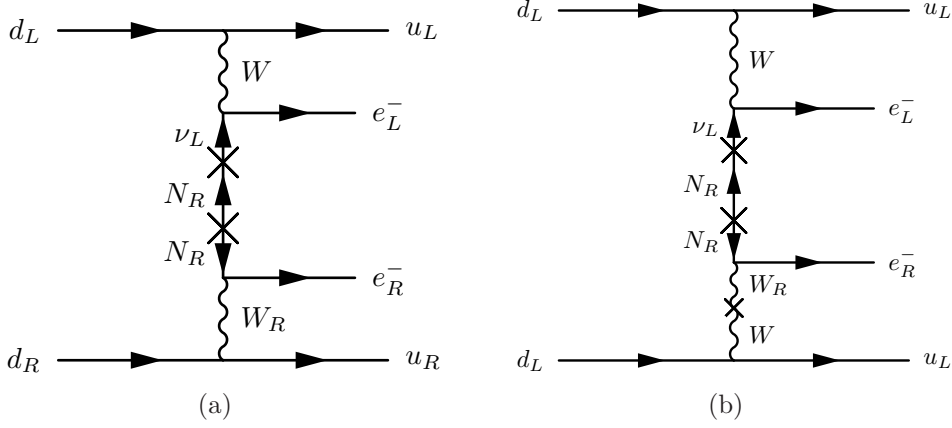
Figure 3: Feynman diagrams of double beta decay in the left-right symmetric model with final state electrons of different helicity: (a) the λ-mechanism and (b) the η-mechanism due to gauge boson mixing.

of the triplet Δ_R and h_{ee} the coupling of the triplet with right-handed electrons.

- Fig. 2(b) is a diagram mediated by the triplet of $SU(2)_L$. The amplitude is given by

$$\mathcal{A}_{\delta_L} \simeq G_F^2 \frac{h_{ee} v_L}{m_{\delta_L^{--}}^2} \, . \tag{12}$$

The diagram is suppressed with respect to the standard light neutrino exchange by at least a factor $q^2/m_{\delta_L^{--}}^2$.

- Fig. 3(a) is a diagram in which the helicities of the final state electrons are different. It is called the λ-diagram, and has an amplitude reading

$$\mathcal{A}_\lambda \simeq G_F^2 \left(\frac{m_{W_L}}{m_{W_R}} \right)^2 \sum_i U_{ei} T_{ei}^* \frac{1}{q} \, ; \tag{13}$$

the particle physics parameter is

$$\eta_\lambda = \left(\frac{m_{W_L}}{m_{W_R}} \right)^2 \left| \sum_i U_{ei} T_{ei}^* \right| \lesssim 9 \times 10^{-7} \, , \tag{14}$$

where T_{ei}^* quantifies the mixing of light neutrinos with right-handed currents [Eq. (A-15)].

- Finally, Fig. 3(b) is another diagram with mixed helicity, possible due to $W_L - W_R$ mixing, which is described by the parameter $\tan\zeta$ defined in Eq. (A-21). The amplitude is

$$\mathcal{A}_\eta \simeq G_F^2 \tan\zeta \sum_i U_{ei} T_{ei}^* \frac{1}{q} \, , \tag{15}$$

with particle physics parameter

$$\eta_\eta = \tan\zeta \left| \sum_i U_{ei} T_{ei}^* \right| \lesssim 6 \times 10^{-9} \,. \tag{16}$$

Note that in both the λ- and η-diagrams there are light neutrinos exchanged (long-range diagrams), and the amplitude is proportional to the mixing matrix $T_{ei}^* = \mathcal{O}(M_D/M_R)$. One therefore needs both a non-zero M_D and $M_R < \infty$, which is illustrated by the Dirac and Majorana mass terms in the propagator. In this case lepton number violation is implicit: the mixing M_D/M_R vanishes for infinite Majorana mass. Ref. [3] gives a detailed explanation of how a complicated cancellation of different nuclear physics amplitudes leads to a limit on the η-diagram that is much stronger than the one on the λ-diagram.

Having written down all interesting diagrams, it is instructive to discuss their expected relative magnitudes. For this naive exercise, let us denote the masses of all particles belonging to the right-handed sector (M_i, W_R and δ_R^{--}) as R. The matrices T and S describing left-right mixing can be written as L/R, where L is about 10^2 GeV, corresponding to the weak scale, or the mass of the W_L. The gauge boson mixing angle ζ is at most of order $(L/R)^2$, and can be much smaller[2]. The mixed λ- and η-diagrams in Fig. 3 are of order $(L/R)^3/q$, whereas the purely right-handed short-range diagrams in Figs. 1(b) (heavy neutrino exchange and right-handed currents) and 2(a) ($SU(2)_R$ triplet exchange and right-handed currents) are of order L^4/R^5. Therefore, with R being of order TeV, the mixed diagrams are expected to dominate by a factor $R^2/(Lq) \sim 10^5$. In the same sense, the amplitudes of the mixed diagrams are also larger than the one for heavy neutrino exchange with left-handed currents (which is proportional to L^2/R^3). Leaving these estimates aside, we continue with a purely phenomenological analysis of the different diagrams at a linear collider.

For this exercise, let us use crossing symmetry to translate the $0\nu\beta\beta$-diagrams from Figs. 1–3 into linear collider cross sections of the form $e^- e^- \to W^- W^-$ (Fig. 4). In each case the two gauge bosons can either have the same polarization ($W_L^- W_L^-$ or $W_R^- W_R^-$), in which case the process can be mediated by either Majorana neutrinos or Higgs triplets, or opposite polarizations ($W_L^- W_R^-$), only possible with the exchange of Majorana neutrinos plus non-zero left-right mixing. Since the limits on W_R are 2.5 TeV [38, 39], diagrams with two W_R are obviously disfavoured. In what regards diagrams with two W_L, both the light and the heavy neutrino exchange can be shown to be suppressed and unobservable, see Ref. [18] for a recent reanalysis. The cross section corresponding to left-handed triplet exchange [Fig. 2(b)] is proportional to $\sqrt{2}v_L h_{ee} = [M_L]_{ee}$ (see Eq. (A-12) and Ref. [35]), so that it is suppressed by light neutrino mass. We are left with diagrams with only one W_R, i.e. the mixed diagrams from Fig. 3. Noting that the limit on the λ-diagram is less stringent by almost two orders

---

[2]See Eq. (A-23) and the comments just below it.
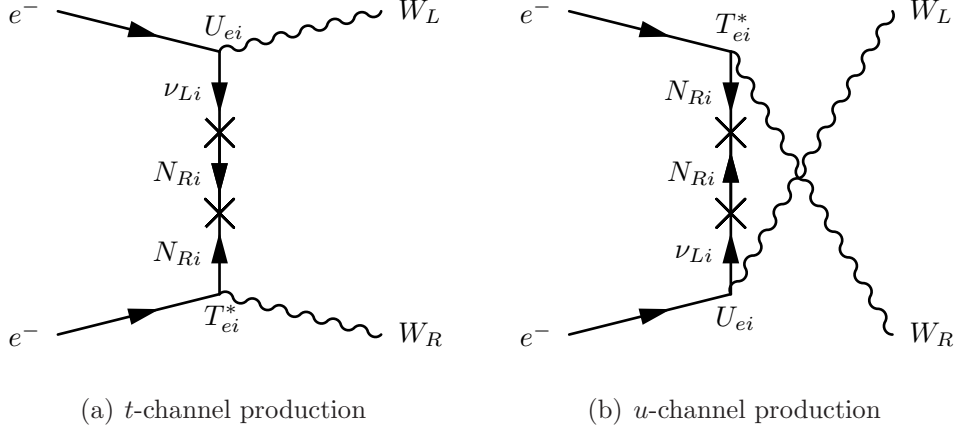
(a) t-channel production (b) u-channel production

Figure 4: Inverse neutrinoless double beta decay diagrams with W_L and W_R in the final state.

of magnitude with respect to the one for η [compare Eqs. (14) and (16)], we are led to the conclusion that the λ-diagram is the most promising channel to study. Fig. 4 shows the relevant Feynman diagram; its cross section will be evaluated in what follows. Let us note here that the SuperNEMO experiment has the possibility to disentangle the λ-diagram from the standard one, because it can probe the angular and energy correlation of the two emitted electrons in $0\nu\beta\beta$ [36]. The mechanism is therefore testable in a variety of ways.

3 Cross section of $e^- e^- \to W_L^- W_R^-$

3.1 Cross section

The two possible channels for the process $e^-(p_1)\, e^-(p_2) \to W_L^-(k_1, \mu)\, W_R^-(k_2, \nu)$ are shown in Fig. 4. Here $p_{1,2}$ and $k_{1,2}$ are the momenta of the particles and μ, ν the Lorentz indices of the W polarization vectors. The matrix element is

$$-i\mathcal{M} = -i\left(\mathcal{M}_t + \mathcal{M}_u\right), \tag{17}$$

where the subscript denotes the t- or u-channel process. In order to evaluate the differential cross section

$$\frac{d\sigma}{d\Omega} = \frac{1}{64\pi^2\, s}\frac{1}{4}|\overline{\mathcal{M}}|^2 \sqrt{\frac{\lambda(s, m_{W_L}^2, m_{W_R}^2)}{\lambda(s, 0, 0)}}, \tag{18}$$

where $\lambda(a, b, c) = a^2 + b^2 + c^2 - 2\,(a\,b + a\,c + b\,c)$, we need

$$|\overline{\mathcal{M}}|^2 = |\overline{\mathcal{M}_t}|^2 + |\overline{\mathcal{M}_u}|^2 + 2\mathrm{Re}\left(\overline{\mathcal{M}_t^*\,\mathcal{M}_u}\right). \tag{19}$$
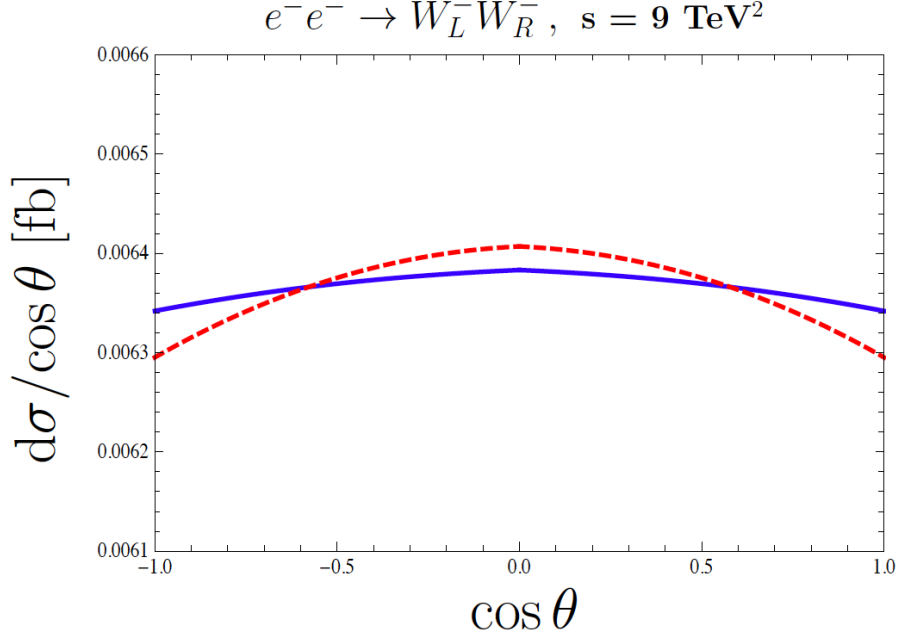
Figure 5: Differential cross section for $e^- e^- \to W_L^- W_R^-$ with $\sqrt{s} = 3$ TeV and for both $m_{W_R} = 2.5$ TeV (dashed red line) and 2.7 TeV (solid blue line), with the latter normalized to facilitate comparison.

The result is (neglecting m_{W_L})

$$
|\overline{\mathcal{M}_t}|^2 = \frac{8\, G_F^2 \, |\sum_i U_{ei} \, T_{ei}^*|^2}{(t - m_i^2)^2} \left(\frac{m_{W_L}}{m_{W_R}}\right)^2 \left\{ 4 m_{W_L}^4 \, m_{W_R}^2 (t - m_{W_R}^2) - t^2 \left[t(s + t) - m_{W_R}^2 (2s + t) \right] \right.
$$

$$
\left. + m_{W_L}^2 \, t \left[4 m_{W_R}^4 + t(2s + t) - m_{W_R}^2 (4s + 5t) \right] \right\},
$$

$$
|\overline{\mathcal{M}_u}|^2 = |\overline{\mathcal{M}_t}|^2 \, (t \leftrightarrow u), \tag{20}
$$

$$
\overline{\mathcal{M}_t^* \, \mathcal{M}_u} \propto \mathrm{Tr}\{ P_R \gamma_\nu \slashed{q}_1 \gamma_\mu \slashed{p}_1 \gamma_\alpha \slashed{q}_2 \gamma_\beta \slashed{p}_2 P_L \} = 0 \, .
$$

The interference term vanishes, since the final state particles are distinguishable. Fig. 5 shows the differential cross section $d\sigma/d\cos\theta$ as a function of $\cos\theta$, for $m_{W_R} = 2.5$ TeV and 2.7 TeV, normalized with respect to each other (the cross section for $m_{W_R} = 2.7$ TeV is actually a factor of two smaller). $d\sigma/d\cos\theta$ is practically flat, and approaches a straight line as m_{W_R} increases.

It is interesting to study the high energy behaviour of the total cross section in the case of light neutrino exchange. In the limit that $\sqrt{s} \to \infty$, the cross section becomes

$$
\sigma(e^- e^- \to W_L^- W_R^-) \simeq \frac{G_F^2 \, m_{W_R}^2}{24\, \pi \, m_{W_L}^2} \, s \, \eta_\lambda^2 \leq 8.8 \times 10^{-5} \left(\frac{m_{W_R}}{\mathrm{TeV}}\right)^2 \left(\frac{\sqrt{s}}{\mathrm{TeV}}\right)^2 \left(\frac{\eta_\lambda}{9 \times 10^{-7}}\right)^2 \mathrm{fb} \, , \tag{21}
$$

where the upper bound on η_λ is given in Eq. (14) and we have neglected the mass of the light neutrinos m_i in the propagator. The apparent violation of unitarity can be explained by taking the full theory into account, in which case the cross section will vanish when $\sqrt{s} \to \infty$ and unitarity is restored (see Appendix B for details).

There is also another diagram analogous to Fig. 4, with heavy neutrinos exchanged. The structure of the matrix elements is the same, we need only to interchange $m_i \leftrightarrow M_i$, $U_{ei} \leftrightarrow V_{ei}^*$
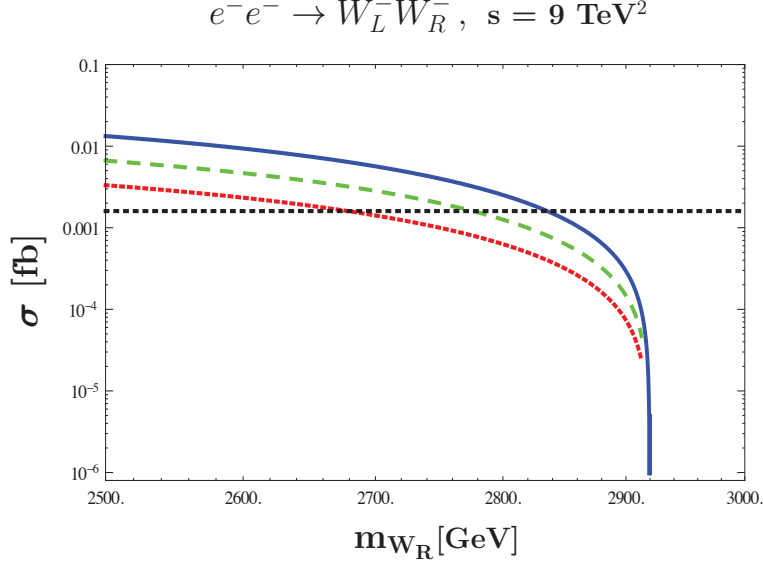
9

$$e^-e^- \to W_L^- W_R^- \; , \quad \mathbf{s = 9 \; TeV^2}$$

Figure 6: Cross section for $e^-e^- \to W_L^- W_R^-$ with $\sqrt{s} = 3$ TeV and three limits for the η_λ parameter: the solid (blue) line is for the current limit $\eta_\lambda = 9 \times 10^{-7}$, the dashed (green) line and the dotted (red) line are for limits on η_λ improved by a factor $\sqrt{2}$ and 2, respectively. The dotted (black) horizontal line corresponds to the cross section that would give five events at an integrated luminosity of 3000 fb^{-1}.

and $T_{ei}^* \leftrightarrow S_{ei}$, where M_i is the mass of the heavy neutrinos and V_{ei}^* and S_{ei} are 3×3 mixing matrices defined in Eq. (A-15). In this case the rate for double beta decay will be suppressed with respect to the case of light neutrino exchange in the λ-diagram.

To calculate the total cross section the limits from $0\nu\beta\beta$ experiments as well as the allowed region for m_{W_R} must be taken into account. Fig. 6 shows the cross section for $e^-e^- \to W_L^- W_R^-$ as a function of m_{W_R} for $\sqrt{s} = 3$ TeV, assuming only light neutrinos are exchanged and with three different limits for η_λ: the solid (blue) line corresponds to the present upper limit [Eq. (14)] given by $0\nu\beta\beta$ experiments, the dashed (green) uses a limit improved by a factor of $\sqrt{2}$ and the dotted (red) line is for a limit improved by a factor of 2. Note that a factor of x improvement in η_λ corresponds to a factor of x^2 improvement in life-time. We also indicate the cross section that would give five events at an integrated luminosity of 3000 fb^{-1} [40], corresponding to a few years of running. It is evident that for 2.5 TeV $\lesssim m_{W_R} \lesssim 2.8$ TeV, enough events are possible in case $0\nu\beta\beta$ is observed soon, and caused by the λ-diagram. Note that since there is no Standard Model background to the process, a small rate is tolerable.

In the next subsection we will show that polarization of the electron beams could be used to enhance the cross section by up to a factor of two. Finally, we should note that in neutrinoless double beta decay different contributions could interfere destructively. In this case the bound on η_λ would be relaxed and a larger cross section is possible.

beam polarization		R
1	2	
0%	0%	1
90% RH	0%	1
50% LH	50% LH	0.75
50% LH	50% RH	1.25
80% LH	50% RH	1.40
90% LH	90% RH	1.81
90% LH	80% RH	1.72
100% LH	100% RH	2

Table 1: Suppression or enhancement factors of the cross section with polarized beams with respect to the unpolarized case.

3.2 Polarized beams

Future linear colliders have the possibility to polarize their beams. In order to quantify the effects on our process, we define the polarization for an electron beam $P_{1,2}$ as follows:

$$P_{1,2} \equiv \frac{N_R^{1,2} - N_L^{1,2}}{N_R^{1,2} + N_L^{1,2}}, \tag{22}$$

where N_R and N_L stand for the number of electrons having right- and left-handed helicity in the electron beam 1 or 2, respectively. If beam 1 is fully left-handed, $P_1 = -1$, whereas for a fully right-handed beam, $P_1 = +1$.

When the electron beam 1 has a polarization of P_1 and the electron beam 2 has a polarization of P_2, the total cross section $\sigma(P_1, P_2)$ of a process is calculated as

$$\sigma(P_1, P_2) = \frac{1}{4} \left\{ (1 - P_1)(1 + P_2)\sigma_{LR} + (1 - P_1)(1 - P_2)\sigma_{LL} \right. \\ \left. + (1 + P_1)(1 + P_2)\sigma_{RR} + (1 + P_1)(1 - P_2)\sigma_{RL} \right\}, \tag{23}$$

where σ_{LR} stands for the cross section of the process when both electron beams are 100% polarized, one left-handed and the other right-handed; σ_{RL}, σ_{LL} and σ_{RR} are defined in a similar way. In our case for the λ-diagram $\sigma_{LL} = \sigma_{RR} = 0$, and σ_{LR} (σ_{RL}) is the cross section that would arise from the t-channel (u-channel) diagram only. Furthermore, $\sigma_{LR} = \sigma_{RL}$. Thus, equation (23) simply becomes

$$\sigma(P_1, P_2) = \sigma(P_2, P_1) = \frac{\sigma_{LR}}{2} (1 - P_1 P_2). \tag{24}$$

Table 1 gives numerical examples. We have defined the ratio R between the cross section of polarized and unpolarized beams:

$$R \equiv \frac{\sigma(P_1, P_2)}{\sigma(0, 0)} = 1 - P_1 P_2. \tag{25}$$

Obviously, $\sigma(0,0)$ is the total cross section calculated before. We see that the event numbers can in principle be doubled. Furthermore, polarization could be used as an additional method to distinguish different mechanisms for processes of the form $e^-e^- \to W^-W^-$. For instance, the process $e^-e^- \to 4$ jets [19] mediated by R-parity violating supersymmetry, involves slepton exchange, which couple mainly to left-handed electrons.

4 Conclusion

We have considered in this paper the process $e^-e^- \to W_L^- W_R^-$ as a clean check of the so-called λ-diagram as the leading contribution to neutrinoless double beta decay. We argued that among the many possible diagrams for $0\nu\beta\beta$ that are possible in left-right symmetric theories, it is the most promising one at a linear collider. Indeed, it may be possible to observe the process at a linear collider with center-of-mass energy of 3 TeV. It is however necessary that both the mass of the W_R and the life-time of $0\nu\beta\beta$ are close to their current experimental limits. We have also considered beam polarization effects and the high energy behaviour of the total cross section, as well as the individual amplitudes.

Appendix

A   Details of the left-right symmetric model

In the left-right symmetric model [41–45], the Standard Model is extended to include the gauge group $SU(2)_R$ (with gauge coupling $g_R \neq g_L$), and right-handed fermions are grouped into doublets under this group. Thus we have the following fermion particle content under $SU(2)_L \times SU(2)_R \times U(1)_{B-L}$:

$$L'_{iL} = \begin{pmatrix} \nu'_i \\ \ell'_i \end{pmatrix}_L \sim (\mathbf{2}, \mathbf{1}, -\mathbf{1}), \quad L'_{iR} = \begin{pmatrix} \nu'_i \\ \ell'_i \end{pmatrix}_R \sim (\mathbf{1}, \mathbf{2}, -\mathbf{1}), \tag{A-1}$$

$$Q'_{iL} = \begin{pmatrix} u'_i \\ d'_i \end{pmatrix}_L \sim (\mathbf{2}, \mathbf{1}, \tfrac{\mathbf{1}}{\mathbf{3}}), \quad Q'_{iR} = \begin{pmatrix} u'_i \\ d'_i \end{pmatrix}_R \sim (\mathbf{1}, \mathbf{2}, \tfrac{\mathbf{1}}{\mathbf{3}}), \tag{A-2}$$

with the electric charge given by $Q = T_L^3 + T_R^3 + \frac{B-L}{2}$ and $i = 1, 2, 3$. The subscripts L and R are associated with the projection $P_{L,R} = \frac{1}{2}(1 \mp \gamma_5)$. In order to break the gauge symmetry and allow Majorana mass terms for neutrinos one introduces the Higgs triplets

$$\Delta_{L,R} \equiv \begin{pmatrix} \delta_{L,R}^+/\sqrt{2} & \delta_{L,R}^{++} \\ \delta_{L,R}^0 & -\delta_{L,R}^+/\sqrt{2} \end{pmatrix}, \tag{A-3}$$

with $\Delta_L \sim (\mathbf{3}, \mathbf{1}, \mathbf{2})$ and $\Delta_R \sim (\mathbf{1}, \mathbf{3}, \mathbf{2})$; the electroweak symmetry is broken by the bi-doublet scalar

$$\phi \equiv \begin{pmatrix} \phi_1^0 & \phi_2^+ \\ \phi_1^- & \phi_2^0 \end{pmatrix} \sim (\mathbf{2}, \mathbf{2}, \mathbf{0}). \tag{A-4}$$

The relevant Lagrangian in the lepton sector is

$$\mathcal{L}_Y^\ell = - \overline{L}_L'(f\phi + g\tilde{\phi})L_R' - \overline{L}_L'^c i\sigma_2 \Delta_L h_L L_L' - \overline{L}_R'^c i\sigma_2 \Delta_R h_R L_R' + \text{h.c.}, \tag{A-5}$$

where $\tilde{\phi} \equiv \sigma_2 \phi^* \sigma_2$; f, g and $h_{L,R}$ are matrices of Yukawa couplings and charge conjugation is defined as

$$\psi_{L,R}^c \equiv \mathcal{C}\overline{\psi}_{L,R}^T, \quad \mathcal{C} \equiv i\gamma_0 \gamma_2. \tag{A-6}$$

If one assumes a discrete LR symmetry in addition to the additional gauge symmetry, the gauge couplings become equal ($g_L = g_R = g$) and one obtains relations between the Yukawa coupling matrices in the model. With a discrete parity symmetry it follows that $h_L = h_R^*$, $f = f^\dagger$, $g = g^\dagger$; with a charge conjugation symmetry $h \equiv h_L = h_R$, $f = f^T$, $g = g^T$.

Making use of the gauge symmetry to eliminate complex phases, the most general vacuum is

$$\langle\phi\rangle = \begin{pmatrix} \kappa_1/\sqrt{2} & 0 \\ 0 & \kappa_2 e^{i\alpha}/\sqrt{2} \end{pmatrix}, \quad \langle\Delta_L\rangle = \begin{pmatrix} 0 & 0 \\ v_L e^{i\theta_L}/\sqrt{2} & 0 \end{pmatrix}, \quad \langle\Delta_R\rangle = \begin{pmatrix} 0 & 0 \\ v_R/\sqrt{2} & 0 \end{pmatrix}. \tag{A-7}$$

After spontaneous symmetry breaking, the mass term for the charged leptons is

$$\mathcal{L}_{\text{mass}}^\ell = -\overline{\ell}_L' M_\ell \ell_R' + \text{h.c.}, \tag{A-8}$$

where the mass matrix

$$M_\ell = \frac{1}{\sqrt{2}}(\kappa_2 e^{i\alpha} f + \kappa_1 g) \neq M_\ell^\dagger \tag{A-9}$$

can be diagonalized by the bi-unitary transformation

$$\ell_{L,R}' \equiv V_{L,R}^\ell \ell_{L,R}, \quad V_L^{\ell\dagger} M_\ell V_R^\ell = \text{diag}(m_e, m_\mu, m_\tau). \tag{A-10}$$

In the neutrino sector we have a type I + II seesaw scenario,

$$\mathcal{L}^\nu_{\text{mass}} = -\tfrac{1}{2}\overline{n'_L}M_\nu n'^c_L + \text{h.c.} = -\tfrac{1}{2}\left(\overline{\nu'_L}\ \overline{\nu'^c_R}\right)\begin{pmatrix} M_L & M_D \\ M_D^T & M_R \end{pmatrix}\begin{pmatrix} \nu'^c_L \\ \nu'_R \end{pmatrix} + \text{h.c.}, \qquad (A\text{-}11)$$

with

$$M_D = \frac{1}{\sqrt{2}}(\kappa_1 f + \kappa_2 e^{-i\alpha}g), \quad M_L = \sqrt{2}v_L e^{i\theta_L}h, \quad M_R = \sqrt{2}v_R h. \qquad (A\text{-}12)$$

Assuming that $M_L \ll M_D \ll M_R$, the light neutrino mass matrix can be written in terms of the model parameters as

$$m_\nu = M_L - M_D M_R^{-1} M_D^T = \sqrt{2}v_L e^{i\theta_L}h - \frac{\kappa_+^2}{\sqrt{2}v_R}h_D h^{-1}h_D^T, \qquad (A\text{-}13)$$

where

$$h_D \equiv \frac{1}{\sqrt{2}}\frac{\kappa_1 f + \kappa_2 e^{-i\alpha}g}{\kappa_+}, \quad \kappa_+^2 \equiv |\kappa_1|^2 + |\kappa_2|^2. \qquad (A\text{-}14)$$

The symmetric 6×6 neutrino mass matrix M_ν in Eq. (A-11) is diagonalized by the unitary 6×6 matrix [46–48]

$$W \equiv \begin{pmatrix} V_L^\nu \\ V_R^\nu \end{pmatrix} = \begin{pmatrix} U & S \\ T & V \end{pmatrix} \simeq \begin{pmatrix} 1_{3\times3} & M_D M_R^{-1} \\ -M_R^{-1*}M_D^\dagger & 1_{3\times3} \end{pmatrix}\begin{pmatrix} U_{\text{PMNS}} & 0 \\ 0 & V_R \end{pmatrix} \qquad (A\text{-}15)$$

to $W^\dagger M_\nu W^* = \text{diag}(m_1, m_2, m_3, M_1, M_2, M_3)$, where the matrices U_{PMNS} and V_R are defined by

$$M_L - M_D M_R^{-1} M_D^T = U_{\text{PMNS}}\,\text{diag}(m_1, m_2, m_3)U_{\text{PMNS}}^T,$$
$$M_R = V_R\,\text{diag}(M_1, M_2, M_3)V_R^T. \qquad (A\text{-}16)$$

The neutrino mass eigenstates $n = n_L + n_L^c = n^c$ are defined by

$$n'_L = \begin{pmatrix} \nu'_L \\ \nu'^c_R \end{pmatrix} = W n_L = \begin{pmatrix} U & S \\ T & V \end{pmatrix}\begin{pmatrix} \nu_L \\ N_R^c \end{pmatrix} \qquad (A\text{-}17)$$

$$n'^c_L = \begin{pmatrix} \nu'^c_L \\ \nu'_R \end{pmatrix} = W^* n_L^c = \begin{pmatrix} U^* & S^* \\ T^* & V^* \end{pmatrix}\begin{pmatrix} \nu_L^c \\ N_R \end{pmatrix}. \qquad (A\text{-}18)$$

Note that the unitarity of W leads to the useful relations

$$V_L^\nu V_L^{\nu\dagger} = UU^\dagger + SS^\dagger = 1 = V_R^\nu V_R^{\nu\dagger} = TT^\dagger + VV^\dagger \quad \text{and} \quad V_L^\nu V_R^{\nu\dagger} = UT^\dagger + SV^\dagger = 0, \quad (A\text{-}19)$$

with the unitary 3×6 matrices $V_L^\nu = (U\ \ S)$ and $V_R^\nu = (T\ \ V)$ defined in Eq. (A-15).

The leptonic charged current interaction in the flavour basis is

$$\mathcal{L}_{CC}^{\mathrm{lep}} = \frac{g}{\sqrt{2}} \left[\overline{\ell'} \gamma^\mu (P_L \cos\zeta - P_R \sin\zeta \, e^{-i\alpha}) \nu' W_{1\mu}^- \right.$$
$$\left. + \overline{\ell'} \gamma^\mu (P_L \sin\zeta \, e^{i\alpha} + P_R \cos\zeta) \nu' W_{2\mu}^- \right] + \text{h.c.}, \tag{A-20}$$

where

$$\begin{pmatrix} W_L^\pm \\ W_R^\pm \end{pmatrix} = \begin{pmatrix} \cos\zeta & \sin\zeta \, e^{i\alpha} \\ -\sin\zeta \, e^{-i\alpha} & \cos\zeta \end{pmatrix} \begin{pmatrix} W_1^\pm \\ W_2^\pm \end{pmatrix} \tag{A-21}$$

characterizes the mixing between left- and right-handed gauge bosons, with $\tan 2\zeta = -\frac{2\kappa_1\kappa_2}{v_R^2 - v_L^2}$. With negligible mixing the gauge boson masses become

$$m_{W_L} \simeq m_{W_1} \simeq \frac{g}{2}\kappa_+, \quad \text{and} \quad m_{W_R} \simeq m_{W_2} \simeq \frac{g}{\sqrt{2}} v_R, \tag{A-22}$$

and assuming that[3] $\kappa_2 < \kappa_1$, it follows that

$$\zeta \simeq -\kappa_1\kappa_2/v_R^2 \simeq -2\frac{\kappa_2}{\kappa_1}\left(\frac{m_{W_L}}{m_{W_R}}\right)^2, \tag{A-23}$$

so that the mixing angle ζ is at most[4] the square of the ratio of left and right scales $(L/R)^2$. The charged current then becomes

$$\mathcal{L}_{CC}^{\mathrm{lep}} = \frac{g}{\sqrt{2}} \left[\overline{\ell'_L} \gamma^\mu \nu'_L W_{L\mu}^- + \overline{\ell'_R} \gamma^\mu \nu'_R W_{R\mu}^- \right] + \text{h.c.}$$
$$= \frac{g}{\sqrt{2}} \left[\overline{\ell_L} \gamma^\mu K_L n_L W_{L\mu}^- + \overline{\ell_R} \gamma^\mu K_R n_L^c W_{R\mu}^- \right] + \text{h.c.} \tag{A-24}$$

Here K_L and K_R are 3×6 mixing matrices

$$K_L \equiv V_L^{\ell\dagger} V_L^\nu, \quad \text{and} \quad K_R \equiv V_R^{\ell\dagger} V_R^{\nu*}, \tag{A-25}$$

connecting the three charged lepton mass eigenstates ℓ_i to the six neutrino mass eigenstates $(\nu_i, N_i)^T$, $(i = 1, 2, 3)$, with [using Eq. (A-19)] $K_L K_L^\dagger = K_R K_R^\dagger = 1$ and $K_L K_R^T = 0$.

Note that in this model one also expects a new neutral gauge boson, Z', which mixes with the standard model Z boson. The mass eigenstates $Z_{1,2}$ have the masses

$$m_{Z_1} \simeq \frac{g}{2\cos\theta_W}\kappa_+, \quad \text{and} \quad m_{Z_2} \simeq \frac{g\cos\theta_W}{\sqrt{\cos 2\theta_W}} v_R, \tag{A-26}$$

where $g = e/\sin\theta_W$ and the $U(1)$ coupling constant is $g' \equiv e/\sqrt{\cos 2\theta_W}$. Again one expects the mixing to be of order $(L/R)^2$. Eqs. (A-22) and (A-26) imply that $m_{Z_2} \simeq 1.7 m_{W_2}$.

---

[3]This is justified if one assumes no cancellations in generating quark masses [49].

[4]Although the experimental limit is $\zeta < 10^{-2}$ [50], for $m_{W_R} = \mathcal{O}(\text{TeV})$ one has $\zeta \lesssim 10^{-3}$ [51]; supernova bounds for right-handed neutrinos lighter than 1 MeV are even more stringent ($\zeta < 3 \times 10^{-5}$) [51–53].

B High energy behaviour of $e^- e^- \to W_L^- W_R^-$

Naively, the high-energy limit of the cross section is obtained by neglecting the neutrino mass in the propagator [see Eq. (20)], i.e.

$$\sigma \propto \left(\sum_i U_{ei} T_{ei}^* \right)^2 , \tag{A-27}$$

which does not seem to vanish. However, one needs to consider the full theory. In calculating the cross section one combines two terms from the Lagrangian in Eq. (A-24):

$$\sum_i \left[\overline{e} \gamma^\mu (K_L)_{ei} P_L n_i W_{L\mu}^- \right] \left[\overline{e} \gamma^\nu (K_R)_{ei} P_R n_i W_{R\nu}^- \right] . \tag{A-28}$$

The identity $\overline{e} \gamma^\nu P_R n_i = -\overline{n_i^c} \gamma^\nu P_L e^c$ allows one to contract $n_i \overline{n_i^c}$ to a propagator, so that in the high energy limit the amplitude is proportional to

$$\sum_i (K_L)_{ei} (K_R)_{ei} = [K_L K_R^T]_{ee} , \tag{A-29}$$

instead of $\sum_i U_{ei} T_{ei}^*$ as in the naive case. As shown in the previous subsection, $K_L K_R^T = 0$, which means that the cross section vanishes in the high energy limit and unitarity is ensured.

C Helicity amplitudes for $e^- e^- \to W_L^- W_R^-$

It is an illustrative exercise to evaluate the helicity amplitudes of the process $e^- e^- \to W_L^- W_R^-$, with the helicity of the electrons and the polarization of the W-bosons fixed. Denoting electron (W-boson) momenta with p_i (k_i), ($i = 1, 2$), the process is

$$e^- (p_1, \lambda_1) \, e^- (p_2, \lambda_2) \to W_L^- (k_1, \tau_1) \, W_R^- (k_2, \tau_2) , \tag{A-30}$$

where $\lambda_{1,2} = \pm \frac{1}{2}$ and $\tau_{1,2} = 0, \pm 1$. Without loss of generality, one can choose p_1 and p_2 to be in the $\pm z$-directions, and assume that the final state particles propagate in the x–z plane. The momenta are then given by

$$p_{1,2}^\mu = (E, 0, 0, \pm E) , \quad k_{1,2}^\mu = (E_{1,2}, \pm |k| \vec{\mathbf{n}}) , \tag{A-31}$$

where $\vec{\mathbf{n}} = (\sin\theta, 0, \cos\theta)$ and

$$E = \frac{\sqrt{s}}{2} , \quad E_{1,2} = \frac{s \pm m_{W_L}^2 \mp m_{W_R}^2}{2\sqrt{s}} , \quad |k| = \frac{\sqrt{\lambda(s, m_{W_L}^2, m_{W_R}^2)}}{2\sqrt{s}} . \tag{A-32}$$

The gauge boson polarization vectors can be defined by

$$\epsilon_{\tau_{1,2}=0}(k_1, k_2) = \pm \frac{1}{m_{W_{L,R}}}\left(\pm|k|, E_{1,2}\sin\theta, 0, E_{1,2}\cos\theta\right),\tag{A-33}$$

$$\epsilon_{\tau_{1,2}=\pm1}(k_1, k_2) = \frac{1}{\sqrt{2}}\left(0, \mp\tau_{1,2}\cos\theta, -i, \pm\tau_{1,2}\sin\theta\right).\tag{A-34}$$

The helicity amplitudes are calculated from

$$\mathcal{M}_{\lambda_1\lambda_2\tau_1\tau_2} = \frac{g^2}{2(t-m_i^2)}\bar{u}(p_1,\lambda_1)\gamma_\mu \slashed{q}\gamma_\nu P_L v(p_2,\lambda_2)\epsilon^{\mu*}(k_1,\tau_1)\epsilon^{\nu*}(k_2,\tau_2)$$

$$+ \frac{g^2}{2(u-m_i^2)}\bar{u}(p_1,\lambda_1)\gamma_\mu \slashed{q}\gamma_\nu P_R v(p_2,\lambda_2)\epsilon^{\mu*}(k_2,\tau_2)\epsilon^{\nu*}(k_1,\tau_1),\tag{A-35}$$

resulting in

$$\mathcal{M}_{\lambda\lambda00} = -\lambda g^2 \frac{\sin\theta\left\{\sqrt{\lambda(s,m_{W_L}^2,m_{W_R}^2)}\left(s+m_{W_L}^2+m_{W_R}^2\right) - 2\lambda\cos\theta\left[\left(m_{W_L}^2-m_{W_R}^2\right)^2 - s^2\right]\right\}}{4m_{W_L}m_{W_R}\left(q^2-m_i^2\right)},$$
$$\tag{A-36}$$

$$\mathcal{M}_{\lambda\lambda0\tau} = \lambda g^2\sqrt{s}\left[(1+2\lambda\tau)\cos^2\frac{\theta}{2} + (1-2\lambda\tau)\sin^2\frac{\theta}{2}\right]$$

$$\times \frac{\cos\theta\left(s+m_{W_L}^2-m_{W_R}^2\right) - 4\lambda\tau m_{W_L}^2 + 2\lambda\sqrt{\lambda\left(s,m_{W_L}^2,m_{W_R}^2\right)}}{2\sqrt{2}m_{W_L}\left(q^2-m_i^2\right)},\tag{A-37}$$

$$\mathcal{M}_{\lambda\lambda\tau0} = -\lambda g^2\sqrt{s}\left[(1-2\lambda\tau)\cos^2\frac{\theta}{2} + (1+2\lambda\tau)\sin^2\frac{\theta}{2}\right]$$

$$\times \frac{\cos\theta\left(s-m_{W_L}^2+m_{W_R}^2\right) + 4\lambda\tau m_{W_L}^2 + 2\lambda\sqrt{\lambda\left(s,m_{W_L}^2,m_{W_R}^2\right)}}{2\sqrt{2}m_{W_L}\left(q^2-m_i^2\right)},\tag{A-38}$$

$$\mathcal{M}_{\lambda\lambda\tau\tau} = g^2\frac{\sin\theta\left[2\lambda\sqrt{\lambda\left(s,m_{W_L}^2,m_{W_R}^2\right)} - 2\lambda\tau\left(m_{W_L}^2-m_{W_R}^2\right) + s\cos\theta\right]}{4\left(q^2-m_i^2\right)},\tag{A-39}$$

$$\mathcal{M}_{\lambda\lambda\tau-\tau} = -\frac{g^2 s\sin\theta(\cos\theta - 2\lambda\tau)}{4\left(q^2-m_i^2\right)},\tag{A-40}$$

$$\mathcal{M}_{\lambda-\lambda00} = \mathcal{M}_{\lambda-\lambda0\tau} = \mathcal{M}_{\lambda-\lambda\tau0} = \mathcal{M}_{\lambda-\lambda\tau\tau} = \mathcal{M}_{\lambda-\lambda\tau-\tau} = 0,\tag{A-41}$$

where $\lambda = \pm\frac{1}{2}$ and $\tau = \pm1$, and $q^2 = t(u)$ when $\lambda = -\frac{1}{2}\left(+\frac{1}{2}\right)$. The amplitude vanishes whenever $\lambda_1 = -\lambda_2$, or in other words, when the two electrons have the same spin (note that one electron is described by a v spinor in Eq. (A-35), which means that its actual helicity is the opposite of the spinor's helicity). The amplitude is only non-zero when the electrons have opposite spin ($\lambda_1 = \lambda_2$); squaring and summing over boson polarizations gives the polarized cross sections σ_{LR} and σ_{RL} in Eq. (23), which correspond to the t- and u-channels respectively.

It is interesting to study the high energy behaviour of these helicity amplitudes. Explicitly,

in the limit $\sqrt{s} \to \infty$ and neglecting neutrino mass one gets

$$\mathcal{M}_{\lambda\lambda00} \xrightarrow{\sqrt{s}\to\infty} -\lambda \frac{g^2 \sin\theta\, s}{2m_{W_L} m_{W_R}},$$

$$\mathcal{M}_{\lambda\lambda0\tau} \xrightarrow{\sqrt{s}\to\infty} -\frac{g^2 \sqrt{s}\left[(1+2\lambda\tau)\cos^2\frac{\theta}{2} + (1-2\lambda\tau)\sin^2\frac{\theta}{2}\right]}{2\sqrt{2}m_{W_L}},$$

$$\mathcal{M}_{\lambda\lambda\tau0} \xrightarrow{\sqrt{s}\to\infty} \frac{g^2 \sqrt{s}\left[(1-2\lambda\tau)\cos^2\frac{\theta}{2} + (1+2\lambda\tau)\sin^2\frac{\theta}{2}\right]}{2\sqrt{2}m_{W_L}}, \qquad \text{(A-42)}$$

$$\mathcal{M}_{\lambda\lambda\tau\tau} \xrightarrow{\sqrt{s}\to\infty} -\lambda g^2 \sin\theta,$$

$$\mathcal{M}_{\lambda\lambda\tau-\tau} \xrightarrow{\sqrt{s}\to\infty} -\lambda\tau \frac{g^2 \sin\theta(1 - 2\lambda\tau\cos\theta)}{1 + 2\lambda\cos\theta}.$$

The amplitudes that contain at least one longitudinally polarized W-boson ($\tau_{1,2} = 0$) are divergent, whereas those with only transverse polarizations ($\tau_{1,2} = \pm 1$) are finite. Summing over fermion spins and boson polarizations gives the result in Eq. (21), and proper consideration of the full theory will lead to a well-behaved total amplitude, in analogy to Appendix B.

References

[1] F. T. I. Avignone, S. R. Elliott, and J. Engel, Rev.Mod.Phys. **80**, 481 (2008), 0708.1033.

[2] J. Gomez-Cadenas et al., Riv.Nuovo Cim. **35**, 29 (2012), 1109.5515.

[3] J. Vergados, Phys.Rept. **361**, 1 (2002), hep-ph/0209347.

[4] W. Rodejohann, Int. J. Mod. Phys. **E20**, 1833 (2011), 1106.1334.

[5] T. G. Rizzo, Phys.Lett. **B116**, 23 (1982).

[6] D. London, G. Belanger, and J. Ng, Phys.Lett. **B188**, 155 (1987).

[7] K. Huitu, J. Maalampi, and M. Raidal, Nucl.Phys. **B420**, 449 (1994), hep-ph/9312235.

[8] T. G. Rizzo, Phys.Rev. **D50**, 5602 (1994), hep-ph/9404225.

[9] P. Helde, K. Huitu, J. Maalampi, and M. Raidal, Nucl.Phys. **B437**, 305 (1995), hep-ph/9409320.

[10] J. Gluza and M. Zralek, Phys.Rev. **D52**, 6238 (1995), hep-ph/9502284.

[11] G. Belanger, F. Boudjema, D. London, and H. Nadeau, Phys. Rev. **D53**, 6292 (1996), hep-ph/9508317.

[12] B. Ananthanarayan and P. Minkowski, Phys.Lett. **B373**, 130 (1996), hep-ph/9512271.

[13] T. G. Rizzo, Int.J.Mod.Phys. **A11**, 1613 (1996), hep-ph/9510349.

[14] C. A. Heusch and P. Minkowski, (1996), hep-ph/9611353.

[15] J. Gluza, Phys.Lett. **B403**, 304 (1997), hep-ph/9704202.

[16] P. Duka, J. Gluza, and M. Zralek, Phys.Rev. **D58**, 053009 (1998), hep-ph/9804372.

[17] J. Maalampi and N. Romanenko, Phys.Rev. **D60**, 055002 (1999), hep-ph/9810528.

[18] W. Rodejohann, Phys. Rev. **D81**, 114001 (2010), 1005.2854.

[19] C. Kom and W. Rodejohann, Phys.Rev. **D85**, 015013 (2012), 1110.3220.

[20] W.-Y. Keung and G. Senjanovic, Phys.Rev.Lett. **50**, 1427 (1983).

[21] A. Ferrari et al., Phys.Rev. **D62**, 013001 (2000).

[22] V. Tello, M. Nemevsek, F. Nesti, G. Senjanovic, and F. Vissani, Phys.Rev.Lett. **106**, 151801 (2011), 1011.3522.

[23] M. Nemevsek, F. Nesti, G. Senjanovic, and V. Tello, (2011), 1112.3061.

[24] B. Allanach, C. Kom, and H. Pas, Phys.Rev.Lett. **103**, 091801 (2009), 0902.4697.

[25] B. Allanach, C. Kom, and H. Pas, JHEP **0910**, 026 (2009), 0903.0347.

[26] CMS Collaboration, CMS-PAS-EXO-11-002 (2011).

[27] ATLAS Collaboration, G. Aad et al., Phys.Lett. **B705**, 28 (2011), 1108.1316.

[28] ATLAS Collaboration, G. Aad et al., (2012), 1203.5420.

[29] F. J. Almeida et al., Eur.Phys.J. **C38**, 115 (2004), hep-ph/0405020.

[30] P. Langacker, Rev.Mod.Phys. **81**, 1199 (2009), 0801.1345.

[31] K. Huitu, J. Maalampi, A. Pietila, and M. Raidal, Nucl.Phys. **B487**, 27 (1997), hep-ph/9606311.

[32] A. Melfo, M. Nemevsek, F. Nesti, G. Senjanovic, and Y. Zhang, Phys.Rev. **D85**, 055018 (2012), 1108.4416.

[33] ATLAS Collaboration, G. Aad et al., Phys.Rev. **D88**, 032004 (2012), 1201.1091.

[34] G. Barenboim, K. Huitu, J. Maalampi, and M. Raidal, Phys.Lett. **B394**, 132 (1997), hep-ph/9611362.

[35] W. Rodejohann and H. Zhang, Phys.Rev. **D83**, 073005 (2011), 1011.3606.

[36] SuperNEMO Collaboration, R. Arnold et al., Eur.Phys.J. **C70**, 927 (2010), 1005.1241.

[37] M. Hirsch, H. V. Klapdor-Kleingrothaus, and O. Panella, Phys. Lett. **B374**, 7 (1996), hep-ph/9602306.

[38] A. Maiezza, M. Nemevsek, F. Nesti, and G. Senjanovic, Phys.Rev. **D82**, 055022 (2010), 1005.5160.

[39] D. Guadagnoli and R. N. Mohapatra, Phys.Lett. **B694**, 386 (2011), 1008.1074.

[40] E. Adli et al., http://project-clic-cdr.web.cern.ch/project-CLIC-CDR/.

[41] R. Mohapatra and J. C. Pati, Phys.Rev. **D11**, 2558 (1975).

[42] J. C. Pati and A. Salam, Phys.Rev. **D10**, 275 (1974).

[43] G. Senjanovic and R. N. Mohapatra, Phys.Rev. **D12**, 1502 (1975).

[44] R. N. Mohapatra and G. Senjanovic, Phys.Rev. **D23**, 165 (1981).

[45] N. Deshpande, J. Gunion, B. Kayser, and F. I. Olness, Phys.Rev. **D44**, 837 (1991).

[46] J. Schechter and J. W. F. Valle, Phys. Rev. **D25**, 774 (1982).

[47] W. Grimus and L. Lavoura, JHEP **0011**, 042 (2000), hep-ph/0008179.

[48] H. Hettmansperger, M. Lindner, and W. Rodejohann, JHEP **1104**, 123 (2011), 1102.3432.

[49] Y. Zhang, H. An, X. Ji, and R. N. Mohapatra, Nucl.Phys. **B802**, 247 (2008), 0712.4218.

[50] Particle Data Group, K. Nakamura et al., J.Phys.G **G37**, 075021 (2010).

[51] P. Langacker and S. U. Sankar, Phys.Rev. **D40**, 1569 (1989).

[52] G. Raffelt and D. Seckel, Phys.Rev.Lett. **60**, 1793 (1988).

[53] R. Barbieri and R. N. Mohapatra, Phys.Rev. **D39**, 1229 (1989).